New & Renewable Energy 2024. 6 Vol. 20, No. 2
ISSN 1738-3935 (Print)
ISSN 2713-9999 (Online)
https://doi.org/10.7849/ksnre.2024.0011
[2024-6-S-WD-001]

Check for updates

Wave Analysis Method for Offshore Wind Power Design Suitable for Ulsan Area

Woobeom Han[1] · Kanghee Lee[2] · Seungjae Lee[3]*

Received 19 March 2024 **Revised** 31 May 2024 **Accepted** 3 June 2024 **Published online** 24 June 2024

ABSTRACT Various loads induced by marine environmental conditions, such as waves, currents, and wind, are crucial for the operation and viability of offshore wind power (OWP) systems. In particular, waves have a significant impact on the stress and fatigue load of offshore structures, and highly reliable design parameters should be derived through extreme value analysis (EVA) techniques. In this study, extreme wave analyses were conducted with various Weibull distribution models to determine the reliable design parameters of an OWP system suitable for the Ulsan area. Forty-three years of long-term hindcast data generated by a numerical wave model were adopted as the analyses data, and the least-squares method was used to estimate the parameters of the distribution function for EVA. The inverse first-order reliability method was employed as the EVA technique. The obtained results were compared among themselves under the assumption that the marginal probability distributions were 2p, 3p, and exponentiated Weibull distributions.

Key words Met-ocean data, Extreme Value analysis, I-FORM, Weibull distribution model, Least squares method

Nomenclature

R^2 : coefficient of determination
$f_{Hs}(h_s)$: probability density function
$F_{Hs}(h_s)$: cumulative distribution function
K : shape parameter
C : scale parameter
γ : location parameter
γ_{EW} : extra shape parameter
$f_{HsTp}(h_s, t_p)$: joint probability distribution
$f_{Hs}(h_s)$: marginal probability distribution of Hs
$f_{Tp \mid Hs}(t_p \mid h_s)$: conditional probability distribution
Hs : significant wave height
Tp : peak period
μ : mean
σ^2 : variance
P : exceedance probability
LSM : least squares Method

Subscript

OWP : offshore wind power
EVA : extreme value analysis
CAPEX : capital expenditure
OWPG : offshore wind power generation
LIDAR : light detection and ranging
ECMWF : european centre for medium-range weather forecast
KIOST : korea institute of ocean science and technology

1) Senior Researcher, Green Energy Research Team, Korea Marine Equipment Research Institute
2) Principal Researcher, Green Energy Research Team, Korea Marine Equipment Research Institute
3) Professor, Division of Naval Architecture and Ocean Systems Engineering, Korea Maritime and Ocean University
***Corresponding author:** slee@kmou.ac.kr
Tel: +82-51-410-4309 Fax: +82-51-403-8305

KHOA : Korea Hydrographic and Oceanographic Agency
MOF : Ministry of Oceans and Fisheries
KMA : korea meteorological administration
GOF : goodness-of-fit
I-FORM : inverse first order reliability method
MAE : mean absolute of error
CRMS : centered root mean squared error
RMSE : root-mean-squared-error
PDF : probability density function
CDF : cumulative distribution function
EC : environmental contour
2p : two - parameter
3p : three - parameter
EC : Environmental contour

1. Introduction

With the recent acceleration of global warming caused by carbon emissions, various such as sea-level rise, extreme droughts, ecosystem destruction, and reduced crop production have become serious concerns. In response, various industries are focusing their efforts on reducing carbon emissions. The energy sector, traditionally reliant on sources like coal, oil, and nuclear power, is transitioning rapidly towards renewable energy. Wind power generation, with its high technological maturity and economic feasibility, is gaining attention as an effective option for reducing carbon emissions.[1]

Compared to land-based wind power generation, OWPG offers numerous advantages, including excellent wind resources and energy generation, ease in developing large-scale wind farms, landscape preservation, and reduced noise. Consequently, a global expansion of OWPG technology is underway.[2] South Korea is also gradually transitioning from land-based wind farms to offshore wind farms. Initiatives include the construction of a 30 MW fixed offshore wind turbine off the northwest coast of Jeju in September 2017 and the completion of a 60 MW offshore wind turbine testbed in the southwest sea in January 2020.

In the ongoing project for Korea's offshore wind farm construction, Jeonnam is advancing an 8.2 GW fixed offshore wind project by 2030. Meanwhile, in Ulsan, multiple global turbine companies and developers are collaborating on a plan to construct a 6 GW floating offshore wind farm off the east coast of Korea.[3]

The construction of wind farms involves several steps, including analyzing marine environmental conditions, predicting the wind power generation capacity, selecting a wind turbine class, and determining design conditions for the wind farm layout and turbine system. Floating offshore wind turbines, unlike fixed ones, require consideration of various external load conditions such as waves, currents, and wind, as they directly impact the turbine system and floating structure's operation and viability. Thus, the collection and analysis of data related to marine environmental conditions are integral components in the construction of offshore wind farms.

Marine environment data, including information on wind, marine conditions, climate, and seabed conditions required for the design of a floating offshore wind turbine system, should be analyzed in accordance with international standards such as IEC61400-3, DNV RP, and ABS.[4]

Marine environment data can be collected as meteorological data from offshore meteorological towers and floating LiDAR equipment. Moreover, to estimate the extreme value of marine conditions with a high reliability using statistical analysis methods, an amount of data corresponding to 1/4 of the return period must be available.[5] However, it is almost impossible to maintain a high recovery rate while monitoring long-term data under extreme marine environment

conditions. Accordingly, in recent years, many researchers have used numerical methods to obtain long-term data such as hindcast.

Sheridan *et al.* (2020) conducted a comparative validation between data collected by two floating LiDAR off the coasts of California, New Jersey, and Virginia and five sets of reanalysis data (MERRA-2, CFSv2, NARR, and RAP) to demonstrate that the ERA5 and RAP models were the most reliable with the lowest wind speed deviation and highest correlation at near surface and hub heights 50-100 m level.[6~13]

Sharmar and Markina (2020) used WAVE WATCH III, a numerical wave model, and various reanalysis wind field models (ERA5, ERA-Interim, NCERP CFSR, and MERRA-2) to validate the reliability of hindcast data. The study compared data collected from offshore buoys and hindcast data generated by various wind field models based on statistical error indices (i.e., normalized bias, scatter index, and root mean square error) and reported that the data generated by ERA5-Wave WATCH III were most similar to actual measured values.[14]

Jeong *et al.* (2016) generated hindcast data in Korean Seas using the SWAN numerical wave model through applying the ECMWF wind field data and conducted a comparative analysis study that compared these data to annual average and peak Hs observation data of the corresponding areas. In that study, Hs time series data were in relatively close agreement and demonstrated a high correlation, but the peak value of hindcast data in high wave areas tended to be under-predicted.[15]

To enhance the quality of hindcast data, it is important to select and apply the wind field model based on whether the objective of the study is a global or regional climate assessment. If it is the latter, a prediction model that can model the climate of the region at high resolution should be used. Recently the KIOST also generated hindcast data suitable for Korean waters using the SWAN numerical wave model and high-resolution WRF wind field model, and Jeong *et al.* (2016) and Eum *et al.* (2020) conducted validation studies on numerical hindcast data model for analyzing marine environment conditions.[15,16] The reliability of the generated hindcast data was validated through a comparison and review against observational data from offshore buoys operated by the KHOA, MOF and KMA; a hindcast database for all Korean sea areas was established based on this approach.

As shown in Fig. 1, the procedures for analyzing external environmental conditions consist of data collection and validation, distribution function model selection, estimation of the parameters of the applicable model, and an analysis of environmental conditions. Up to present, most researchers have used the Weibull distribution, which has characteristics similar to an energy distribution with a low frequency of extreme

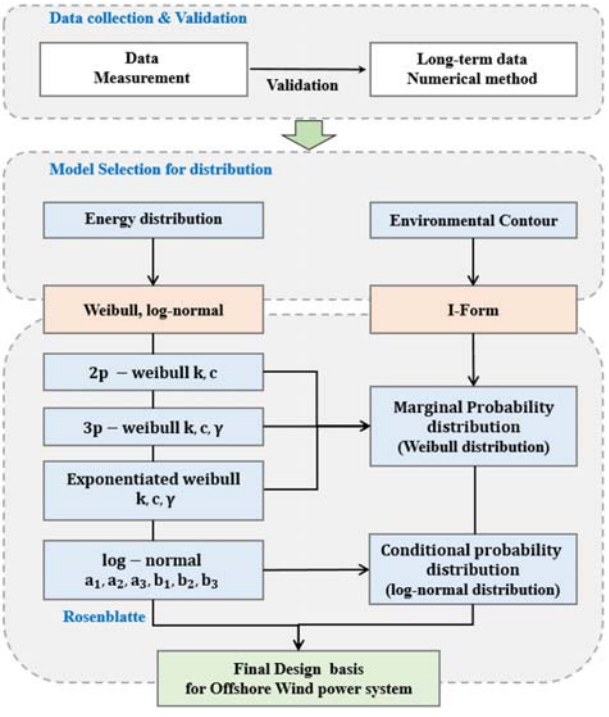

Fig. 1. A procedure for analyzing external environmental conditions

values and high frequency of low values, when analyzing the marine environment. Weibull distributions can be divided into 2p, 3p, and exponentiated Weibull distributions according to the composition of parameters, and recently, Pobočíková *et al.* (2023) compared the characteristics of these distributions based on wind data from the Poprad region in Slovakia. The wind data were compared by months and seasons using six types of GOF testing methods, and the study results indicated that the exponentiated Weibull distribution was most similar to the collected wind data as it provided relatively high flexibility.[17]

The Gumbel function and I-FORM are widely used as the main methods for estimating extreme values. The Gumbel function is used to estimate the extreme value of a single variable, whereas I-FORM is used to estimate the extreme value of two or more combined variables. More specifically, with I-FORM, marine conditions with combinations of various external conditions acting on them can be combined to be expressed as a limit state. Accordingly, international standards such as IEC61400-3 Annex G, DNVGL-RP-C205, and NORSOK actively recommend the use of I-FORM in OWP turbine system design. The Gumbel function and I-FORM have the same purpose of use for extreme value estimation. However, as shown in Fig. 1, I-FORM differs in that it considers two or more variables to represent a critical limit state and design point.

Recently, Park *et al.* (2020) used wind, wave, and current data collected from the Barents Sea hindcast data to estimate the parameters of 2p and 3p Weibull distributions, which were then used to perform EVA using I-FORM. EVA using the parameters of the 2p Weibull distribution showed values similar to the collected data, but that of the 3p Weibull distribution showed overestimated results.[18]

An existing study by Pobočíková *et al.* (2023) reported that the exponentiated Weibull distribution was the most suitable model under normal wind conditions, but the study did not perform an additional analysis under extreme wind conditions. Moreover, the extreme condition analysis study by Park *et al.* (2020) presented analysis results that evaluated only the 2p and 3p Weibull distributions, and not the exponentiated Weibull distribution.

In the present study, marine environment data from the Ulsan sea area in Korea were used to calculate return period values necessary for designing floating OWP systems. The data collected from a marine meteorological buoy comprised short-term data spanning six years. However, due to insufficient quantity, these data were not suitable for use in EVA. Therefore, long-term hindcast data were employed instead and validity of the data was confirmed by comparing hindcast data with measured data from buoys. The parameters of the Weibull distribution were estimated using LSM, and checked for reliability by comparison with the CDF of the measured data. To derive a method suitable for extreme condition analysis in the Ulsan sea area of South Korea, this study additionally included the exponentiated Weibull distribution, which was not previously considered in the study conducted by Park *et al.* (2020).

This study proposes the most appropriate Weibull distribution model for extreme value analysis. This is demonstrated by comparing the error rates between the maximum value observed in the hindcast data and the estimated extreme values. Through this comprehensive procedure, we provide the extreme values of Hs and Tp that are essential for the accurate design of an offshore wind system in the waters off Ulsan, Korea.

2. Marine environment data

2.1 Collection of marine environment observation data

Marine environment observation data were acquired over a six years period (January 1, 2016 to December 31, 2021) using a marine meteorological buoy operated by KMA. The marine meteorological buoy is located at 35°20′43.00″N, 129°50′29.00″E, approximately 43 km off the coast of Daesong-ri, Ulsan. This location is suitable for acquiring marine environment data because there is no interference from nearby topography, landmarks, and reefs. Detailed information about the site coordinate, instrument, data recovery rate, monitoring period, measurement time interval, and observed items is provided in Table 1.

Table 1. Marine environment buoy monitoring conditions

Site coordinate	35°20′43.00″N, 129°50′29.00″E
Instrument	Buoy
Data recovery rate	Wind speed – 92.71% (48773/52608) Significant wave height – 95.17% (50069/52608)
Period	1/1/2016 – 12/31/2021
Time interval	1hour
Items	Wind speed at 10 m height Wind direction at 10 m height Significant wave height Wave direction

2.2 Marine environment hindcast data collection

KIOST has generated hindcast data using a WRF wind field and SWAN numerical wave model that includes wind-induced wave generation, wave dissipation, three-wave nonlinear interactions, and four-wave nonlinear interactions. In the present study, data from hindcast database developed by KIOST were used for comparison and validation against the buoy observation data. The location had coordinates of 35°19′58.78″N, 129°40′1.17″E, which is approximately 15 km from the buoy. Detailed information is given in Table 2 and Fig. 2.

Table 2. Marine environment monitoring condition of hindcast data

Site coordinate	35°19′58.78″N, 129°40′1.17″E
Period	1/1/1979 – 12/31/2021
Time interval	1hour
Monitoring period	1/1/2016 – 12/31/2021
Measurement time interval	1hour
Items	Wind speed at 10 m height Wind direction at 10 m height Significant wave height Wave direction Peak-period

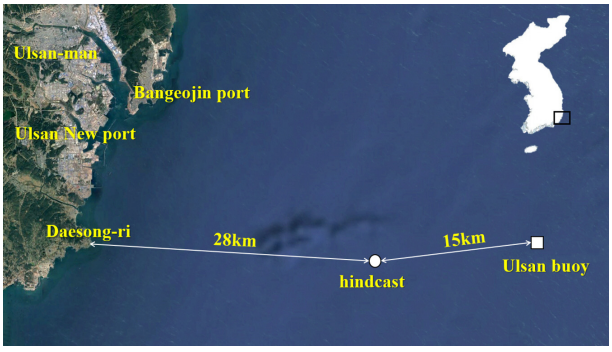

Fig. 2. Locations of observation buoy and hindcast data

2.3 Data Validation

The wind speed and Hs observation data collected by the marine meteorological buoy between 2016 and 2021 and hindcast data for the same period were compared and analyzed to test the validity of the data. The characteristics of the hindcast data were reviewed using a time series validation and the hourly and daily R^2 and error metrics were calculated to quantitatively analyze the accuracy between the model estimated values and observed values. Typical error metrics include bias, MAE, CRMS, and RMSE, which can be defined by Eq.(1)–(4) as follows:[19]

$$\text{Bias} = \frac{1}{N}\Sigma_{i=1}^{N}(V_{mod,i} - V_{obs,i}) \quad (1)$$

$$\text{MAE} = \frac{1}{N}\Sigma_{i=1}^{N}|V_{mod,i} - V_{obs,i}| \quad (2)$$

$$\text{CRMSE} = \sqrt{\frac{1}{N}\Sigma_{i=1}^{N}\left[(V_{mod,i} - \overline{V_{mod}}) - (V_{obs,i} - \overline{V_{obs}})\right]^2} \quad (3)$$

$$\text{RMSE} = \sqrt{\frac{1}{N}\Sigma_{i=1}^{N}(V_{mod,i} - V_{obs,i})^2} \quad (4)$$

where, N is the number of data points; Vmod and Vobs represent estimates from the hindcast data and buoy-observed values, respectively, and $\overline{V_{mod}}$ and $\overline{V_{obs}}$ represent the mean value of each data. Bias indicates the mean deviation between the model estimate and observed value, MAE indicates the mean of all absolute errors of the estimates and observed values, RMSE indicates the mean root square of estimation error, and CRMSE indicates the difference in variation of the estimate and observed value based on the center of the error.

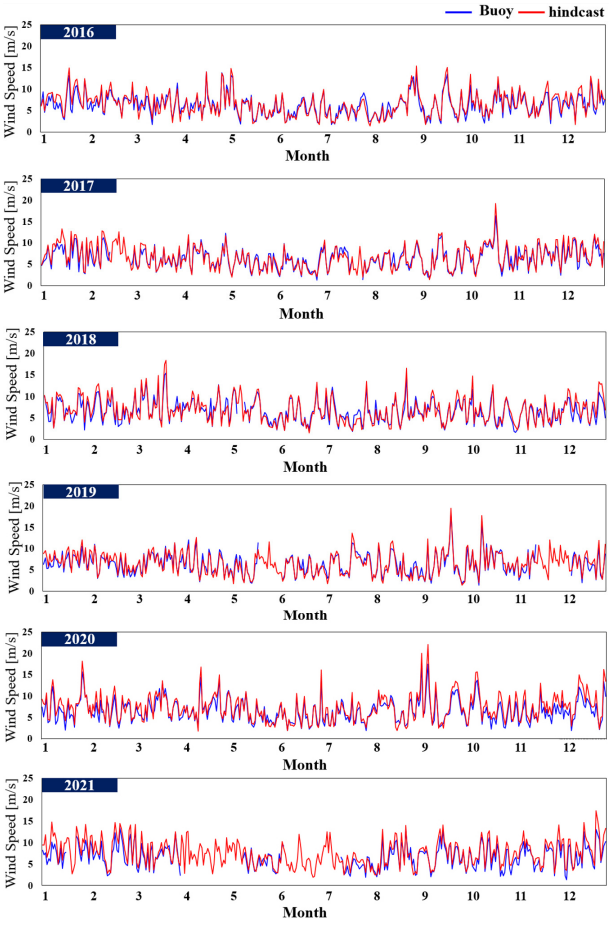

Fig. 3. Time series of hindcast data wind speed and buoy-observed wind speed

2.3.1 Validation of hindcast data characteristics

Fig. 3 shows the time series data for daily average wind speed of buoy-observed data and hindcast data collected at the same times between 2016 and 2021.

The results for the time series comparison of daily

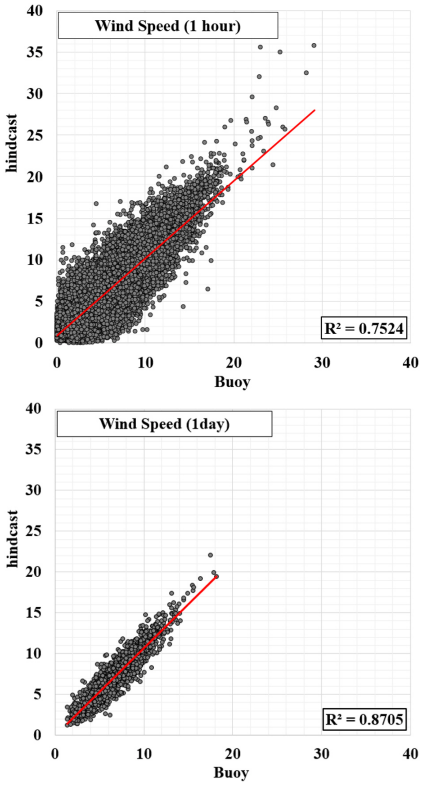

Fig. 4. Coefficients of determination (R^2) of wind speed

Table 3. Error metric result of wind speed

Item	Wind speed (1hour)	Wind speed (1day)
Bias	0.45 m/s	
MAE	1.39 m/s	0.89 m/s
CRMSE	1.76 m/s	1.07 m/s
RMSE	1.82 m/s	1.16 m/s

hindcast and observed data showed generally high similarity. However, the hindcast data values tended to show localized under– or over–estimation in some intervals, as compared to the observed values. To perform a more precise assessment of data reliability, hourly and daily wind speed data were quantitatively analyzed, and the results are shown in Table 3. The results of 1day average data show a relatively lower error rate as compared to 1hour raw data. These results were the product of errors, with the large local variability being offset as 1hour raw data were averaged. Fig. 4 shows the R^2 of the 1hour raw wind data and 1day average wind data. The probability of data occurrence over 15 m/s high wind speed intervals was relatively low, but the hindcast data values tended to be over–estimated relative to the observed values.

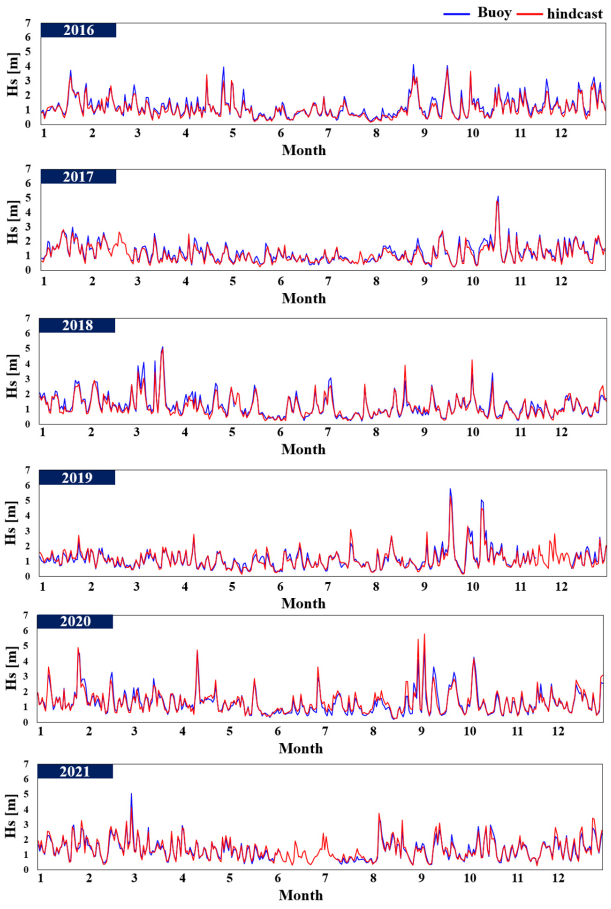

Fig. 5. Time series of hindcast data Hs and buoy–observed Hs

Fig. 5 shows the time series data for 1day average Hs from the observed and hindcast data collected during the same period between 2016 and 2021. Overall, the similarity of Hs data was high. In significant wave height under 3 m, the hindcast data values tended to be under–estimated during the entire observation period, except 2020. Table 4 shows the quantitative analysis results.

Fig. 6 shows the R^2 of 1hour Hs raw data and 1day Hs average data. These values demonstrated a similarity higher reliability as compared to the wind speed data.

Table 4. Error metric result of wind speed

Item	Hs (1hour)	Hs (1day)
Bias	−0.04 m/s	
MAE	0.212 m/s	0.161 m/s
CRMSE	0.296 m/s	0.217 m/s
RMSE	0.298 m/s	0.221 m/s

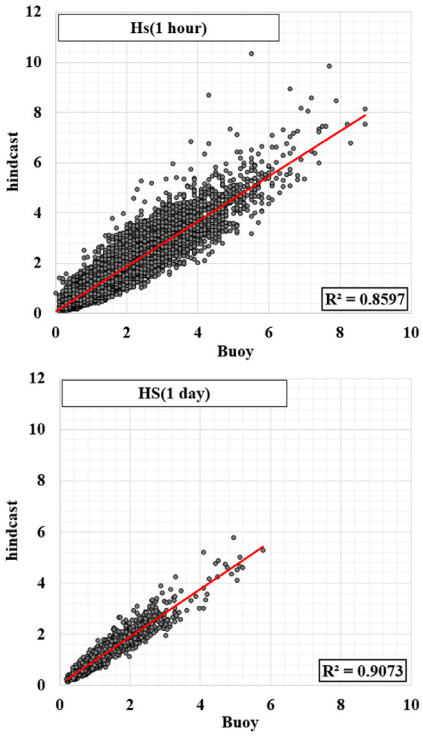

Fig. 6. Coefficients of determination (R^2) of significant wave height

3. Statistical analysis methods

Probability distributions and parameters selected for statistical analysis may have a significant impact on the reliability of analysis of marine environment conditions. Energy sources such as waves, currents, and wind exhibit frequency distributions that closely resemble the Weibull distribution. Therefore, the Weibull distribution is widely used in the marine field to analyze environmental conditions. Moreover, because OWP and offshore structures exhibit external environmental characteristics that combine two or more variables (i.e., wind speed–turbulence intensity, wave height–wave period, and so on), estimating extreme values using I–FORM is recommended. For example, the wave height found at a specific wave period may be higher than the wave height found under the longest wave period condition; in such a case, the wave load generated at that wave period could have an even greater impact on the response of the structure.

3.1 Weibull distributions (2p, 3p, and exponentiated)

The most used 2p Weibull distribution can be expressed as a PDF; $f_{H_s}(h_s)$ and a CDF; $F_{H_s}(h_s)$, as shown in Eq.(5) and (6) below:[20]

$$f_{H_s}(h_s)=\frac{k}{c}\left(\frac{h_s}{c}\right)^{k-1}\cdot\exp\left[-\left(\frac{h_s}{c}\right)^{k}\right] \tag{5}$$

$$F_{H_s}(h_s)=1-\exp\left[-\left(\frac{h_s}{c}\right)^{k}\right] \tag{6}$$

Where, hs is the significant wave height, k is the shape parameter, and c is the scale parameter. In the 3p Weibull distribution, the location parameter γ is added, and the distribution can be expressed by Eq. (7) and (8). In the exponentiated Weibull distribution, the extra shape parameter γ_{EW} is added and the distribution can be expressed by Eq.(9) and (10).

$$r_{H_s}(h_s)=\frac{k}{c}\left(\frac{h_s-\gamma}{c}\right)^{k-1}\cdot\exp\left[-\left(\frac{h_s-\gamma}{c}\right)^{k}\right] \tag{7}$$

$$F_{H_s}(h_s)=1-\exp\left[-\left(\frac{h_s-\gamma}{c}\right)^{k}\right] \tag{8}$$

$$r_{H_s}(h_s)=\frac{\gamma_{Ew}k}{c}\left(\frac{h_s}{c}\right)^{k-1}\cdot\exp\left[-\left(\frac{h_s}{c}\right)^{k}\right]\cdot \left\{1-\exp\left[-\left(\frac{h_s}{c}\right)^{k}\right]\right\}^{\gamma_{EW}-1} \tag{9}$$

$$F_{H_s}(h_s)=\left\{1-\exp\left[-\left(\frac{h_s}{c}\right)^{k}\right]\right\}^{\gamma_{EW}} \tag{10}$$

The k is a factor that determines the shape of the curve, with a small k value indicating an evenly distributed energy source and increasing k values showing a narrow curve width and increase in the inflection point. The value of the c tends to increase with a higher average energy source. In addition, parameters γ and γ_{EW} added in the 3p or exponentiated Weibull distribution help control the shape of the tails of Weibull distribution. These parameters are used to produce and determine the Weibull distribution models suitable for specific environmental conditions.

LSM was used to estimate the Weibull distribution parameters. By taking the log of both sides of Eq. (6), known as the Weibull CDF, the equation was arranged as a first–order expression as shown in Eq. (11).

$$\ln\left\{\ln\left[\frac{1}{1-F_{H_s}(h_s)}\right]\right\}=k\ln h_s-k\ln c \tag{11}$$

Where, $\ln\left\{\ln\left[\frac{1}{1-F_{H_s}(h_s)}\right]\right\}$ represents the dependent variable y, whereas k represents the slope of independent variable x, $\ln h_s$ represents the independent variable x, and klnc represents the y–intercept. The parameter values were calculated by first–order

regression analysis on the first-order equation. For 3p and exponentiated Weibull distributions, parameters with a R^2 value closest to 1 were selected as γ and γ_{EW}.

3.2 Extreme value analysis of inverse first order reliability method

I-FORM, first proposed by Winterstein is an EC method that effectively approximates the limit state of a given return period.[21] This method is used in various fields, including offshore structure design, natural disaster prediction, and environmental risk analysis. Eq. (12) shows the joint probability distribution of Hs and the peak period, which can be expressed as the product of marginal probability distribution of Hs and conditional probability distribution of corresponding peak period, respectively.

$$f_{H_s T_p}(h_s, t_p) = f_{H_s}(h_s)\, f_{T_p|H_s}(t_p|h_s) \tag{12}$$

Where, $f_{H_s}(h_s)$ is the marginal probability distribution of Hs, $f_{T_p|H_s}(t_p|h_s)$ is the conditional probability distribution, HS is the significant wave height, and Tp is the peak period. Generally, $f_{H_s}(h_s)$, the marginal probability distribution of Hs (assumed to be a Weibull distribution), can be defined by Eq. (13), whereas $f_{T_p|H_s}(t_p|h_s)$, the conditional probability distribution of the peak period (assumed to be a log-normal distribution), can be defined by Eq. (14).

$$f_{H_s}(h_s) = \frac{k}{c}\left(\frac{h_s}{c}\right)^{k-1} \exp\left[-\left(\frac{h_s}{c}\right)^{k}\right] \tag{13}$$

$$f_{T_p|H_s}(t_p|h_s) = \frac{1}{t_p \sigma \sqrt{2\pi}} \exp\left[\frac{-(\ln(t_p)-\mu)^2}{2\sigma^2}\right] \tag{14}$$

Where, k, c, μ, and σ^2 represent the shape parameter, scale parameter, mean, and variance, respectively, and when a 3p or exponentiated Weibull distribution is used on the marginal probability distribution, parameter γ or γ_{EW} is added.

Eq. (15) and (16) define parameters μ and σ^2 of the conditional probability distribution used in a log-normal distribution; these are determined by $E[\ln(t_p)]$ and $VAR[\ln(t_p)]$ corresponding to each interval of Hs. Parameters a1, a2, a3, b1, b2, and b3 are estimated by a non-linear fitting method.[22]

$$\mu = a_1 + a_2 \cdot h_s^{a_3} \tag{15}$$

$$\sigma^2 = b_1 + b_2 \cdot \exp[-h_s \cdot b_3] \tag{16}$$

I-FORM, based on the conventional structural reliability approach, is a method for determining the exceedance probability according to the return period and corresponding response level. All variables are independent and follow a Gaussian distribution. The order by which I-FORM is used to derive the contour line is as follows.[23]

[Step 1] The exceedance probability (P) of a given return period can be derived by Eq. (17).

$$P[X > x] = 1 - F(x|\mu, \sigma) \tag{17}$$

[Step 2] The probability of condition $P[X > x]$ can be derived by Eq. (18), whereas Eq. (19), representing an inversed Gaussian cumulative

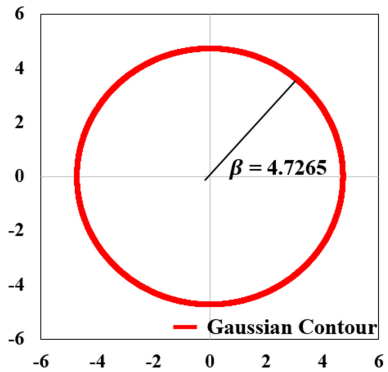

Fig. 7. U-space of 100year return period

distribution, can be applied to derive the radius of U-space (β) with mean of 0 and standard deviation of 1, as shown in Fig. 7.

$$P[X > x] = F(x|\mu, \sigma) \tag{18}$$

$$\beta = x = F^{-1}(p|0, 1) \tag{19}$$

[Step 3] Parameters of Weibull (k, c) and log-normal distributions (a_1, a_2, a_3, b_1, b_2, b_3) are estimated using Eq. (11), (15), and (16).

[Step 4] Eq. (20) and (21), transformation formulas proposed by Rosenblatt, can be used to transform U-space into a physical parameter space, the target response level, is found as the highest value on the surface in the physical parameter space.[24]

$$F(\mu_1) = 1 - \exp\left[-\left(\frac{h_s}{c}\right)^k\right] \tag{20}$$

$$F(\mu_2) = \frac{1}{2} + \frac{1}{2} erf\left[\frac{\ln(t_p) - \mu(h_s)}{\sqrt{2\sigma(h_s)}}\right] \tag{21}$$

h_s can be defined by Eq. (22)-(24) depending on the parameters that comprise the Weibull distribution, whereas T_p corresponding to h_s can be defined by Eq. (25).

$$h_{s(2p\ Weibull)} = c[-\ln 1 - F(\mu_1)]^{\frac{1}{k}} \tag{22}$$

$$h_{s(3p\ Weibull)} = c[-\ln 1 - F(\mu_1)]^{\frac{1}{k}} + \gamma \tag{23}$$

$$h_{s(Exponentiated)} = c\left[-\ln 1 - F(\mu_1)^{\frac{1}{\gamma_{EW}}}\right]^{\frac{1}{k}} \tag{24}$$

$$t_p = \exp\left[\left(\sqrt{\sigma \cdot \mu_2}\right) + \mu\right] \tag{25}$$

μ and σ^2 of the conditional probability distribution can be derived by Eq. (15) and (16).

The methods for extracting data used in I-FORM can be divided into the global approach, which uses all data measured over a long period, and the event approach, which extracts only data that exceed a certain.[25] The hindcast data used in the present study represent 43years of data, and because there was sufficient data, the global approach was chosen.

4. Extreme wave condition analysis of East Sea of Korea

Floating OWP systems that are exposed to various external environmental conditions require a system optimization design that incorporates the site characteristics, including wind, waves, and currents. Wave conditions can prominently cause stress and fatigue load on the floating structure and act as a key factor that determines the dynamic response and motion performance of the structure. Accordingly, international standards, such as DNV-GL and ABS, recommend that the I-FORM statistical approach should be used for designing offshore structures to incorporate the extreme values of Hs for a return period of 100years and corresponding Tp in the design. An estimation of incorrect extreme value can cause the under- or over-design of an offshore structure, which can have a negative impact on its structural integrity and economic feasibility. Accordingly, to assure the reliability of extreme value estimation, a series of extreme wave analyses was conducted with various Weibull distribution models applied to I-FORM.

Fig. 8 shows the results from estimating the parameters of 2p, 3p, and exponentiated Weibull distributions using LSM. The exponentiated Weibull distribution and hindcast data were in close accordance.

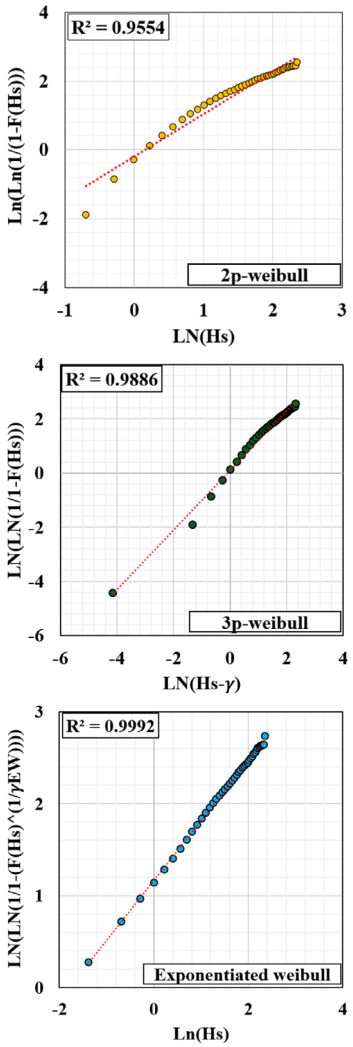

Fig. 8. Coefficients of determination of significant wave height for Weibull distribution parameters

Table 5. Parameters for Weibull distribution

Parameter	2p	3p	Exp
K	1.459	1.105	0.654
C	1.487	0.926	0.168
γ or γ_{EW}	–	0.234	14.216

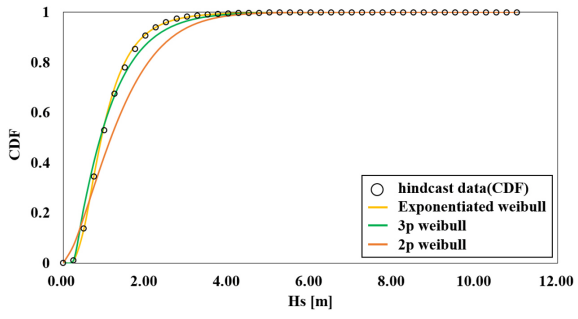

Fig. 9. CDF of hindcast data and each Weibull distribution

The parameter results are shown in Table 5.

The CDF were compared to verify the estimated values of the parameters. The results of which are shown in Fig. 9. The exponentiated Weibull CDF closely resembled hindcast data at all intervals, whereas the 3p Weibull distribution showed similar results in some intervals between Hs greater than or equal to 1m and less than or equal to 1.5 m. In contrast, the 2p Weibull distribution showed over-estimations in intervals between Hs greater than or equal to 0 m and less than or equal to 0.5 m and under-estimations in intervals of Hs greater than 0.5 m, with slight differences in all intervals.

The conditional probability distribution applied in I-FORM was determined by $E[\ln(t_p)]$ and $VAR[\ln(t_p)]$ of Tp corresponding to Hs. The distribution of Hs typically demonstrated high frequency and narrow scatter in low-wave intervals, and thus, it was important to reproduce the distribution characteristics by setting the bin spacing to be small. Accordingly, the bin of Hs was set to 0.25 m, and the $E[\ln(t_p)]$ and $VAR[\ln(t_p)]$ of Tp corresponding to this value were calculated. Parameters a_1, a_2, a_3, b_1, b_2, and b_3 were derived by non-linear fitting using Eq. (15) and (16), the results of which are shown in Table 6 and Fig. 10.

The error rates of peak Hs of hindcast data and estimated extreme values were calculated to validate the reliability of the I-FORM EVA results. Relative to the peak Hs value of hindcast data, EVA results larger than that value were expressed as "+" and results smaller than that value were expressed as "–," as shown in Table 7.

The results from I-FORM EVA using the parameters

Table 6. Estimation of conditional probability distribution parameters

a1	a2	a3	b1	b2	b3
0.03	1.62	0.175	0	0.059	0.485

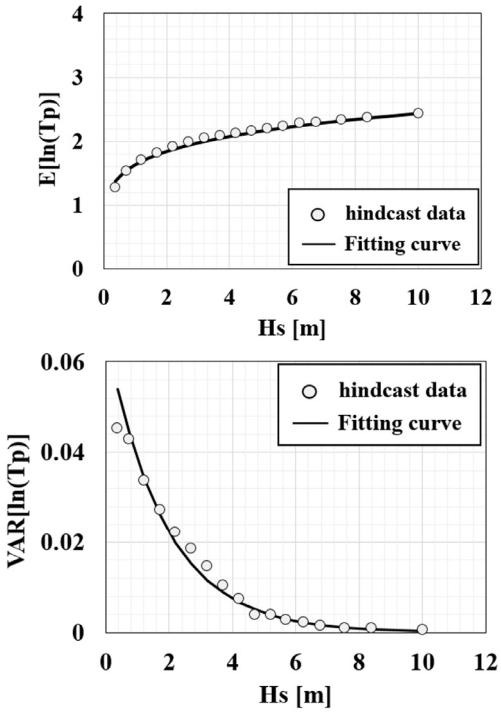

Fig. 10. Estimation of conditional probability distribution parameters

Table 7. Comparison of extreme values (I-form vs hindcast data)

Parameter	Extreme value		Error rate [%]	
	Hs [m]	Tp [s]	Hs [m]	Tp [s]
hindcast	10.7	11.58	-	
2p	8.56	10.88	-20.00	-6.04
3p	9.56	11.4	-10.65	-1.55
Exp	11.15	12.17	+4.21	+5.09

of the exponentiated Weibull distribution overestimated Tp. However, the error rates of Hs and Tp were within 5%, showing a higher accuracy than the 2p and 3p Weibull distributions. The results from I-FORM EVA using the parameters of the 2p and 3p Weibull distributions underestimated Hs and Tp as compared to hindcast data, whereas Hs showed a large error rate of at least 10%.

Fig. 11 represents the results of each probability of exceedance on a log scale, demonstrates the the exponentiated Weibull distribution has the best agreement with the hindcast, indicating the highest reliability

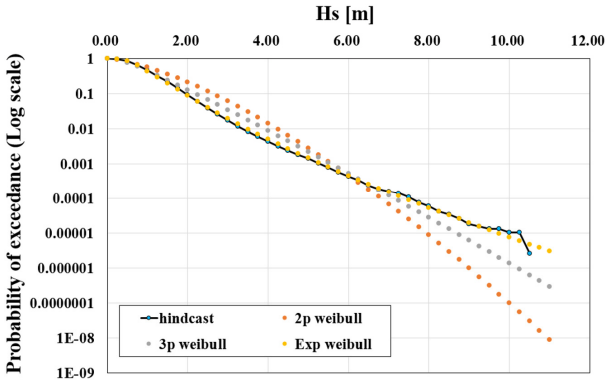

Fig. 11. Comparison on probability of exceedance (Log sacle)

in the I-FORM estimation results. Based on such findings, the exponentiated Weibull distribution was confirmed to most accurately reproduce the extreme value distribution characteristics of waves and is identified as the most suitable model for EVA.

Fig. 12 shows the contour of 1, 10, 20, 43, 50, and 100years by combining the parameters of 2p, 3p, and exponentiated Weibull distributions. Table 8 shows the extreme values by return period derived by the I-FORM contour. Relative to the extreme values obtained by applying exponentiated Weibull distribution, the extreme value of Hs for a return period of 100 years was 12.09 m/s, and the corresponding Tp was 12.61s.

5. Conclusion

This study confirmed the high similarity between the hindcast data and measured data, demonstrating that hindcast data is an effective alternative to collecting long-term measured data. In particular, the estimation of extreme value using the exponentiated Weibull distribution showed an error rate of less than 5%, exhibiting the highest accuracy in the Ulsan seas of South Korea. Future research aims to improve the reliability of extreme value estimation by combining

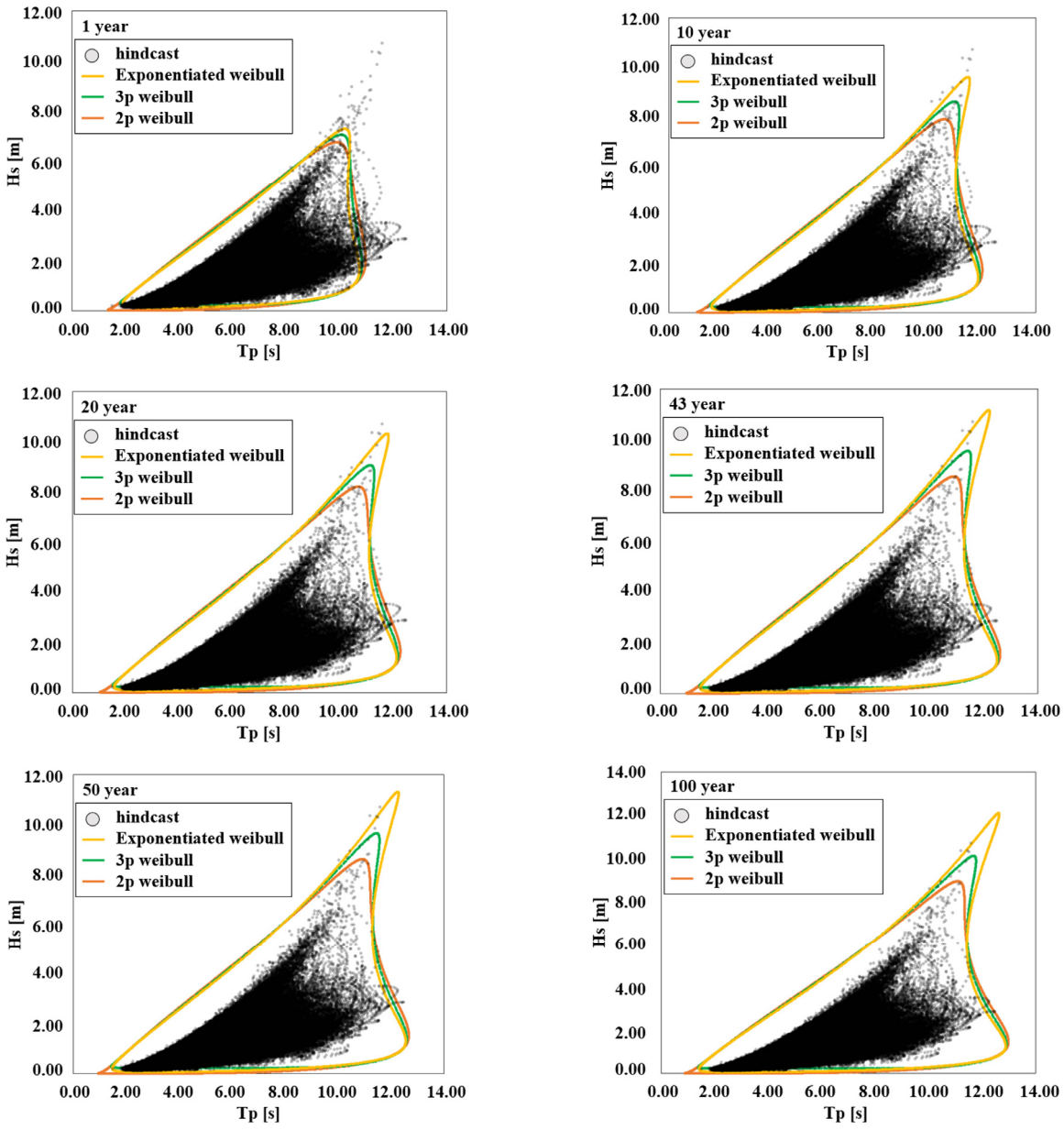

Fig. 12. Environmental contours for significant wave height and peak period

Table 8. Return value for waves (Tp, Hs)

year	2p		3p		Exp	
	Tp [s]	Hs [m]	Tp [s]	Hs [m]	Tp [s]	Hs [m]
1	9.4	6.75	10.05	7.05	10.19	7.29
10	10.51	7.88	10.90	8.60	11.41	9.59
20	10.69	8.20	11.14	9.06	11.77	10.32
43	10.88	8.56	11.40	9.56	12.17	11.15
50	10.91	8.62	11.45	9.66	12.25	11.32
100	11.08	8.94	11.67	10.11	12.61	12.09

multiple EC methods and parameter estimation techniques.

Acknowledgment

This work was supported by by the Ministry of Trade, Industry and Energy, (MOTIE) and the Korea Energy Technology Evaluation and Planning (KETEP) [Grant Number: 20228520020020].

References

[1] Olabi, A.G., Obaideen, K., Abdelkareem, M.A., AlMallahi, M.N., Shehata, N., Alami, A.H., Mdallal, A., Hassan, A.A.M., and Sayed, E.T., 2023, "Wind energy contribution to the sustainable development goals: Case study on London array", Sustainability., **15**(5), 4641.

[2] Barooni, M., Ashuri, T., Velioglu Sogut, D., Wood, S., and Ghaderpour Taleghani, S., 2023, "Floating offshore wind turbines: Current status and future prospects", Energies, **16**(1), 2.

[3] AEGIR., PONDERA., and COWI., 2021, "Accelerating South Korean offshore wind through partnerships: A Scenario-based study of supply chain, levelized cost of energy and employment effects", https://www.rvo.nl/sites/default/files/2021/06/Accelerating%20Offshore%20Wind%20South%20Korea%20May%202021.pdf.

[4] Ko, D.H., Jeong, S.T., Cho, H., and Kang, K.S., 2014, "Extreme offshore wind estimation using typhoon simulation", J. Korean Soc. Coast. Ocean Eng., **26**(1), 16-24.

[5] Isobsen, I., 2005, "Petroleum and natural gas industries-Specific requirements for offshore structure-Part 1: Metocean Design and Operating Conditions", British Standard Institute, 19901-19901.

[6] Sheridan, L.M., Krishnamurthy, R., Gorton, A.M., Shaw, W.J., and Newsom, R.K., 2020, "Validation of reanalysis-based offshore wind resource characterization using lidar buoy observations", Web. mar technol soc j., **54**, 44-61.

[7] Gelaro, R., McCarty, W., Suárez, M.J., Todling, R., Molod, A., Takacs, L., Randles, C.A., Darmenov, A., Bosilovich, M.G., and Reichle, R., *et al*., 2017, "The modern-era retrospective analysis for research and applications, version 2 (MERRA-2)", J. Clim., **30**, 5419-5454.

[8] Saha, S., Moorthi, S., Wu, X., Wang, J., Nadiga, S., Tripp, P., Behringer, D., Hou, Y.T., Chuang, H.Y., and Iredell, M., *et al.,* 2011, "The NCEP climate forecast system version 2 (CFSv2) 6-hourly products", Research Data Archive at the National Center for Atmospheric Research, Computational and Information Systems Laboratory, **10**, Dp. D61C1TXF.

[9] Saha, S., Moorthi, S., Wu, X., Wang, J., Nadiga, S., Tripp, P., Behringer, D., Hou, Y.T., Chuang, H.Y., and Iredell, M., *et al.,* 2014, "The NCEP climate forecast system version 2", J. Clim., **27**(6), 2185-2208.

[10] Mesinger, F., DiMego, G., Kalnay, E., Mitchell, K., Shafran, P.C., Ebisuzaki, W., Jović, D., Woollen, J., Rogers, E., and Berbery, E.H., *et al.,* 2006, "North American regional reanalysis (NARR)", Bull. Amer. Meteor. Soc., **87**, 343-360.

[11] Hersbach, H., Bell, B., Berrisford, P., Hirahara, S., Horányi, A., Muñoz-Sabater, J., Nicolas, J., Peubey, C., Radu, R., and Schepers, D., *et al*., 2020, "The ERA5 global reanalysis", Quart. J. Royal Meteorol. Soc., **146**(730), 1999-2049.

[12] Benjamin, S.G., Weygandt, S.S., Brown, J.M., Hu, M., Alexander, C.R., Smirnova, T.G., Olson, J.B., James, E.P., Dowell, D.C., and Grell, G.A., *et al*., 2016, "A North American hourly assimilation and model forecast cycle: The rapid refresh", Mon. Weather Rev., **144**(4), 1669-1694.

[13] Sheridan, L.M., Krishnamurthy, R., García Medina, G., Gaudet, B.J., Gustafson, W.I., Mahon, A.M., Shaw, W.J., Newsom, R.K., Pekour, M., and Yang, Z., 2022, "Offshore reanalysis wind speed assessment across the wind turbine rotor layer off the United States Pacific coast", Wind Energ. Sci., **7**(5), 2059-2084.

[14] Sharmar, V., and Markina, M., 2020, "Validation of global wind wave hindcasts using ERA5, MERRA2, ERA-Interim and CFSRv2 reanalyzes", IOP Conf. Ser.: Earth Environ. Sci., **606**, 012056.

[15] Jeong, W., Oh, S., and Eum, H.S., 2016, "Analysis of wave climate around Korea based on long-term hindcast and coastal observation data", J. Coast. Res. Spec., **75**(sp1), 735-739.

[16] Eum, H.-S., Jeong, W.-M., Chang, Y.S., Oh, S.-H., and Park, J.-J., 2020, "Wave energy in Korean Seas from 12-year wave hindcasting", J. Mar. Sci. Eng., **8**(3), 161.

[17] Pobočíková, I., Michalková, M., Sedliačková, Z., and Jurášová, D., 2023, "Modelling the wind speed using exponentiated Weibull distribution: Case study of Poprad-Tatry, Slovakia", Appl. Sci., **13**(6), 4031.

[18] Park, S.B., Shin, S.Y., Shin, D.G., Jung, K.H., Choi, Y.H., Lee, J., and Lee, S.J., 2020, “Extreme value analysis of metocean data for Barents Sea”, J. Ocean Eng. Technol., **34**(1), 26-36.

[19] Draxl, C., Hodge, B.M., Clifton, A., and McCaa, J., 2015, “ Overview and meteorological validation of the wind integration national dataset toolkit. technical report”, National Renewable Energy Laboratory, https://doi.org/10.2172/1214985.

[20] Mathew, S., 2006, “Wind energy: fundamentals, resource analysis and economics”, Springer, 68-78.

[21] Winterstein, S.R. Ude, T.C., Cornell, C.A., Bjerager, P., and Haver, S., 1993, “Environmental parameters for extreme response: Inverse form with omission factors”, Proc. ICOSSAR-93, Innsbruck, Austria, 551-557.

[22] Morken, M.H., 2014, “A comparison of various approaches for predicting extreme wave induced response for design of offshore structures”, M.S. thesis, University of Stavanger, Norway.

[23] Harver, S., and Winterstein, S.R., 2008, “Environmental contour lines: A method for estimating long-term extreme by a short-term analysis”, Trans. Soc. J. Nav. Archit. Mar. Eng., **116**, 116-127.

[24] Rosenblatt, M., 1952, “Remarks on a multivariate transformation”, Ann. Math. Statist., **23**(3), 470-472.

[25] Bitner-Gregersen, E.M., 2015, “Joint met-ocean description for design and operations of marine structures”, Appl. Ocean Res., **51**, 279-292.